Chinese Journal of Polar Science, Vol 17, No 2, 117 - 123, December 2006

Amery ice shelf DEM and its marine ice distribution

Wang Yafeng(王亚凤)[1], Wen Jiahong(温家洪)[1], Liu Jiying(刘吉英)[1], Kenneth C. Jezek[2], and Beata M. Cathso[2]

1 Department of Geography, Shanghai Normal University, Shanghai 200234, China;

2 Byrd Polar Research Center, The Ohio State University, Columbus, OH 43210, USA

Received November 20, 2006

Abstract The Amery Ice Shelf is the largest ice shelf in East Antarctica. A new DEM was generated for this ice shelf, using kriging to interpolate the data from ICESat altimetry and the AIS-DEM. The ice thickness distribution map is converted from the new DEM, assuming hydrostatic equilibrium. The Amery Ice Shelf marine ice, up to 230 m thick, is concentrated in the northwest of the ice shelf. The volume of the marine ice is 2.38×10^3 km^3 and accounts for about 5.6% of the shelf volume.

Key words ICESat GLAS, DEM, Marine ice, Amery Ice Shelf, Antarctica

1 Introduction

The Amery Ice Shelf, the largest ice shelf in East Antarctica, has a total surface area of about 6.1×10^4 km^2. The ice shelf drains the grounded ice from the interior of the Lambert Glacier drainage basin that covers an area of larger than 1.3×10^6 km^2, and discharges at the ice shelf front, which is less than 200 km, or about 1/60 of the Antarctic coastline (Fricker *et al.* 2000a). Therefore, the Lambert Glacier-Amery Ice Shelf system is active and sensitive to global climate and sea level change.

Fricker *et al.* (2000b) generated a 1km cell-size digital elevation model (DEM) for the Amery Ice Shelf (AIS-DEM) from the European Space Agency's European Remote Sensing Satellite (ERS-1) radar altimeter waveform data. The ERS-1 satellite provides measurements ranging from 82°N to 82°S. The radar altimeter has a sensor footprint of 2.4 km. The separation of neighboring ground tracks was 2 - 3 km on the Amery Ice Shelf. The AIS-DEM doesn't cover the Amery Ice Shelf completely while it has relatively larger errors around the southern grounding line. The estimations of distribution and thickness of the marine ice beneath the ice shelf by Fricker *et al.* (2001) also have larger uncertainties due to errors of the geoidal model they used (Fricker HA 2005, personal communication).

The National Aeronautics and Space Administration (NASA) launched an Ice, Cloud and Elevation Satellite (ICESat) with a Geoscience Laser Altimeter System (GLAS) in January 2003 (Fan *et al.* 2005). The ICESat GLAS data have a sensor footprint of 70 m, and a typical along-track spacing between footprints is 170 m on the ground. The ICESat data is more accurate than radar altimeter data, which provides measurements ranging from

86°N to 86°S. We generate a 1km cell-size DEM with high accuracy for the Amery Ice Shelf, using kriging to interpolate the data from ICESat altimetry and the AIS-DEM.

Basal melting and refreezing are significant components of the mass budget of ice stream systems and ocean-ice interaction. We generate the distribution maps of the ice thickness and marine ice over the Amery Ice Shelf using the new DEM, which provides important data for the research of mass budget of Lambert Glacier-Amery Ice Shelf system and for the processes of basal melting/refreezing and ocean dynamics research. In this paper we will introduce our data resources, interpolation methods, present and discuss results of marine ice distribution over the Amery Ice Shelf.

2 DEM

We generate a more accurate and integrated Amery Ice Shelf DEM by using geostatistical analyzing function of ArcGIS to interpolate the data from ICESat GLAS data and the AIS-DEM.

2.1 *Datasets*

The datasets we used in this study include: (1) The ICESat GLAS altimetry data (Zwally *et al* 2003): release number (18–22), operation period (L1, L2a-2c, L3a-3c), collected between 2003 spring to 2004 winter. The footprint of ICESat altimetry is 70 m, a typical along-track spacing between footprints is 170 m, and an across-track separation ranges from 2 to 30 km. (2) AIS-DEM (Fricker *et al* 2000b): a 1km cell-size digital elevation model (DEM) for the Amery Ice Shelf. The altimeter datasets were collected during two geodetic phases of ERS-1 (phase E and F, orbit number 14302–19247) between April 1994 and March 1995. (3) The Amery Ice Shelf outline data (Wen *et al* 2006). We basically adopted the dataset provided by Fricker *et al* (2000b), modified using several datasets, including the southern grounding line position of the Amery Ice Shelf mapped by InSAR (Rignot 2002); velocities with a spacing interval of 400 by 400 m derived from the Modified Antarctic Mapping Mission (MAMM) InSAR project (Jezek 2003), and a RADARSAT coherence image map. (4) The OSU91a geoid model (Jezek 1999). It is used to convert data from ellipsoidal to orthometric height. The difference between OSU91a geoid and WGS84 is −67 m to +42 m in Antarctica.

2.2 *Data preprocessing*

Firstly we define a rectangle to be the DEM's extent, which is 600 km long and 245 km wide, covering the entire Amery ice shelf and its neighborhood with higher elevations. ICESat data have totally 4.2202×10^5 points, which are imported into ArcGIS from dBASE Ⓥ file and its projection is defined as Polar Stereographic projection. The ICESat GLAS data have a smaller along-track spacing between footprints with a very large across-track separation. Such spacing shares the same distribution properties with many other geographical or geological data surveys that are carried out from vehicles that follow tracks, i.e., the data are densely sampled along tracks while the flight tracks themselves are widely spaced. Such a distribution poses serious difficulties for most interpolation techniques and results in a directional bias in the grid (Lythe and Vaughan 2001). To counter this, we reprocessed the data. The method is that the rectangle covering the Amery Ice Shelf is divided into 1 km grids. The total number of grids is 1.47×10^5. The mean elevation value of ICESat altimeter data within each grid can be calculated, using the spatial analyzing function of ArcGIS (Zonal statistics), and then the mean elevation values are linked with the centroid of each grid. The original data points are lessened from 4.2202×10^5 to 1.9634×10^4.

2.3 Interpolation

The method used to interpolate the ICESat altimeter data to create a DEM is kriging. This is a geostatistical technique that produces a statistically unbiased, minimum error-variance data estimate at unobserved points of a surface from a set of observed points, provided that surface has spatially stationary statistics. The model of the semivariogram is used in combination with the observed data to calculate estimates of the surface elevation at the grid nodes. Kriging is known as an "exact interpolator" because it maintains the data values at each of the observed points (Deutsch and Journel 1992).

The ICESat data are ellipsoidal height, and should be converted to orthometric heights relative to the OSU91A geoid (Liu *et al.* 1999). When the DEM was generated, ICESat and ERS data (i.e. if a grid doesn't contain ICESat data, we use AIS-DEM data instead) were used inside the Amery Ice Shelf while only the ICESat data were used beyond the margin of the ice shelf. The new DEM is showed in Figure 1.

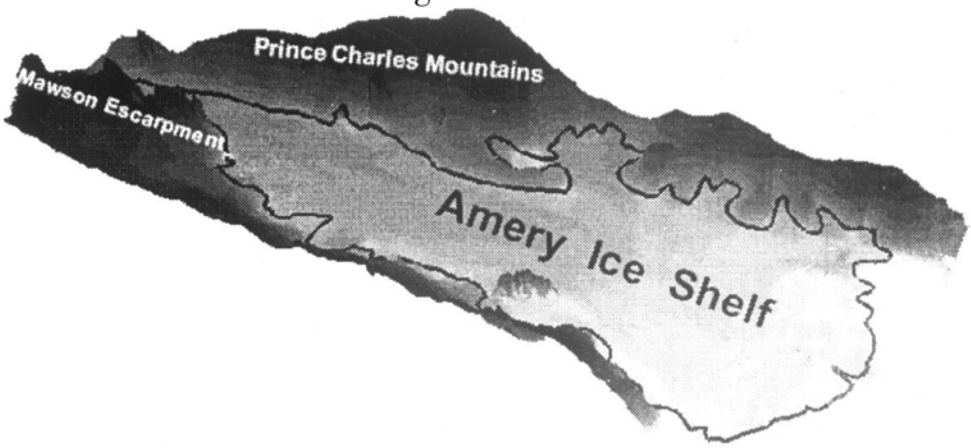

Fig. 1 The Amery Ice Shelf digital elevation model

The periphery of Amery ice shelf is mountains with an elevation reaching up to 500–700 m. The mean height of the ice shelf is about 82 m. The elevation descends from 270 m to 40m from south to north along a central stream line. The ice shelf surface is not very smooth, ridging as stripes resulted from large glaciers such as Lambert, Fisher and Mellor that drain into the ice shelf from the interior basin.

3 Marine ice layer

Brine rejects during sea ice formation at the surface freezing point, T_{f0} (~ −1.9℃), which produces dense High Salinity Shelf Water (HSSW). The HSSW descends beneath the Amery Ice Shelf to the deep southern grounding line (about 2000– 3000 m). Pressure suppresses the melting point by 1.9℃ below T_{f0} (Rignot and Jacobs 2002), so that the HSSW is able to efficiently melt ice. The resulting fresh, buoyant ISW rises following the slope of the ice shelf base and passes along the gradient in the pressure melting point, causing it to supercool at some depth. This leads to the refreezing that produces a layer of marine ice beneath the Amery Ice Shelf.

For a freely floating ice shelf, the relationship between the surface height H (relative to sea level) and the thickness Z at any point is given by the hydrostatic equation:

$$H = \frac{Z(\rho_w - \rho_i)}{\rho_w}$$

The hydrostatic condition is satisfied over most of the ice shelf as far as 73.2°S. Where ρ_w and ρ_i is the column-averaged densities of sea water and ice respectively. ρ_w is equal to 1.029×10^3 km m^{-3} (Wong *et al.* 1998). Wen *et al.* (2006) present the column-averaged ice density over the Amery Ice Shelf. The density distribution includes three portions, 921 to 914.7 kg m^{-3} between 0 (the southern grounding line) and 215 km, 914.7 to 903.5 kg m^{-3} between 215 and 315 km, and 903.5 to 890.5 kg m^{-3} from 315 km to the ice front.

Ice thickness (Z) of the Amery ice shelf is converted from the new DEM (H). Then the marine ice thickness can be educed by the ice thickness (Z) and RES (radio-echo sounding) data. RES system typically detects the meteoric-marine ice boundary, since it exhibits a moderate dielectric contrast but the signal may not penetrate the marine ice layer itself because of high absorption of electromagnetic energy within (Blindow 1994). So the marine ice thickness can be educed by the ice thickness (Z) subtracting the meteoric ice thickness, which is collected by the RES system. RES data is downloaded from http: //www.antarctica.ac.uk/aedc/bedmap/ (Lythe *et al.* 2001).

4 Results and discussion

Our results show that the Amery Ice Shelf marine ice is up to 230 m thick, mean thickness is 90.4 m, area is 2.64×10^4 km^2, which was concentrated in the northwest of the ice shelf. The volume of the marine ice is 2.38×10^3 km^3 and accounts for about 5.6% of the shelf volume. The southern boundary of the marine ice is 71.6°S, which continuously extends to the ice front.

There are several sources of error in our estimate of marine ice thickness. The OSU91a geoid model which used to convert data from ellipsoidal to orthometric height is not reliable in Antarctica due to the paucity of gravity measurements. Geoid errors may be up to 3 m. Errors in RES data arise from uncertainty in the speed of radio waves in ice and firn, navigation errors, and limitations digitizing RES film records (Vaughan *et al.* 1993). The RMS of ice thickness differences at intersections of RES flight lines in the northwest part of the shelf is 26 m. The error of ice density model is about 5 kg m^{-3} (Wen *et al.* 2006). Combining all errors, our estimated marine ice layer thickness has an uncertainty of about 30m. An access hole through the shelf was drilled by ANARE at AM01 (69.442°S, 71.417°E) in 2001/02. The firn and grounding ice thickness is 40 m and 270 m respectively (Allison 2003). The marine ice thickness approximately is 210 m, which is from 270 m to 480 m.

The marine thickness according to our marine ice distribution map at this location (AM01) is 173 ±30 m, roughly consistent with upper limit of the measurement of ANARE. Fricker *et al.* (2001) estimated the marine ice was up to 190 m thick and accounted for about 9% of the shelf volume. The measurement at AM01 shows that the maximum of the marine ice thickness over the ice shelf exceeds 190 m. The actual value is obviously larger than the estimation of Fricker *et al.* (2001).

RES records shows strong basal echoes under the eastern side (south of 71.3°S) and under the southern ice shelf from which we infer basal melting. The implied distribution of melting and freezing results from a three-dimensional ocean circulation under the AIS that is clockwise in the x-y plane, combined with a vertical sub-ice-shelf thermohaline component. The marine ice distribution in Fig. 2 is consistent with accretion zones obtained from modelling the three-dimensional ocean circulation beneath the Amery Ice Shelf (Williams *et al.* 1998). The thickest marine ice occurs in the two longitudinal bands, oriented along the ice flow direction. These are located each side of the Charybdis/Scylla glacier inflow where this stream merges with some unnamed glaciers. Marine ice preferentially accretes in troughs formed under thinner ice at the margins of these streams.

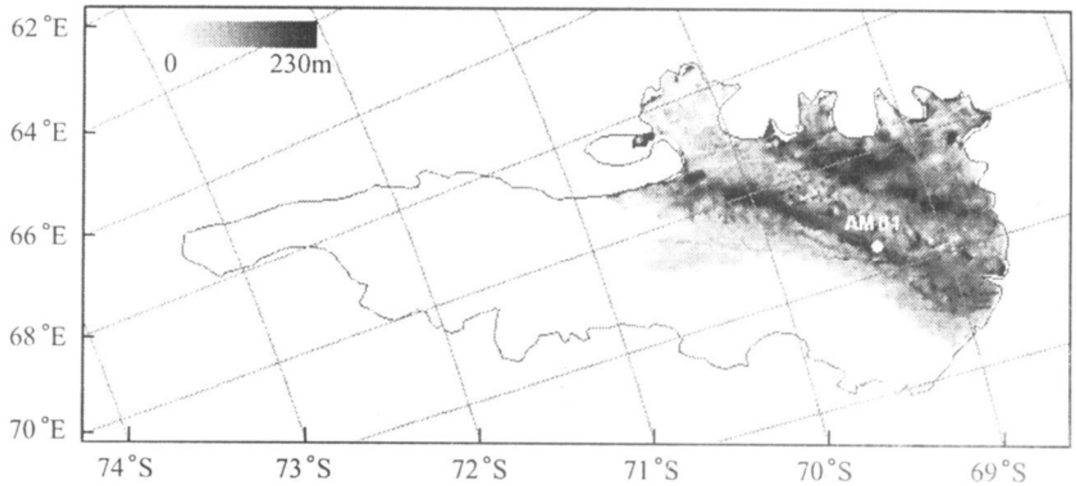

Fig. 2 Distribution of the marine ice beneath the Amery Ice Shelf

We compared this pattern of marine ice accretion with that occurring under the Ronne Ice Shelf. The maximum of AIS marine ice thickness is 230 m, compared to 140 m for the Filchnner Ice Shelf (Grosfeld *et al.* 1998) and 350 m for the Ronne (Thyssen *et al.* 1993). However, the estimated thickness of marine ice under the Ross Ice Shelf is less than 10 m (Neal 1986). This variation between ice shelves is most likely due to a combination of the different cavity geometries, especially the ice shelf drafts, and the different water properties and circulations. The Amery Ice Shelf has a long, narrow, sub-ice-shelf cavity with a maximum draft of about 2200 m. The Filcher and Ronne ice shelves also have deep drafts (about 1400 m), whereas the Ross Ice Shelf has a shallower draft (about 800 m) and a smaller length-to-width ratio. Under the Filchner and Ronne Ice Shelves, a warm sub-shelf current melts the marine ice layer before it reaches the calving front (Thyssen *et al.* 1993). Green icebergs from the Amery Ice Shelf, which have capsized since calving thus revealing the marine ice, have been observed in Prydz Bay and further west (Warren *et al.* 1993).

5 Concluding remarks

In this paper we generate a 1 km cell-size new DEM for the Amery Ice Shelf with high accuracy by using kriging to interpolate the data from ICESat altimetry and the AIS-DEM. The marine ice thickness is educed by the ice thickness obtained by hydrostatic equilibrium subtracting the meteoric ice thickness collected by the RES system, which provides the important conditions for modeling the processes of ocean-ice interaction. Basal melting and freezing are significant components of the mass budget of the Amery Ice Shelf. It is expected that their rates and distribution will change with any warming-induced perturbation to the present sub-ice-shelf thermohaline circulation (Wang *et al.* 2006). Continued monitoring of the AIS marine ice thickness will not only increase the accuracy of the mass budget, but also provide an indicator of change in the ocean conditions and early signs of major structural change in the ice shelf itself.

Acknowledgements This work is supported by National Natural Science Foundation (40471028, 40231013) and Shanghai Shu Guang Project (05SG46). We thank the Science Computing Faculty of the Ohio State University for providing the ICESat GLAS data, with T. Yoon's kind assistance, and Dr. Helen A. Fricker for providing us with the AIS-DEM.

References

Allison I (2003): The AMISOR project: ice shelf dynamics and ice-ocean interaction of the Amery Ice Shelf, FRISP Report, No. 14.

Blindow N (1994): The central part of the Filchner-Ronne Ice Shelf, Antarctica: internal structures revealed by 40MHZ monopulse RES. Annals of Glaciology, 20: 365–371.

Deutsch C, Journel A (1992): GSLIB geostatistical software library and user's guide. Oxford, Oxford University Press.

Fan CB, Li JC, Wang D *et al.* (2005): Application of ICESat to Geoscience research. Journal of Geodesy and Geodynamics, 25(2): 94–97.

Fricker, HA, Warner RC, and Allison I (2000a): Mass balance of the Lambert Glacier-Amery Ice Shelf system, East Antarctica: a comparison of computed balance fluxes and measured fluxes, Journal of Glaciology, 46(155): 561–570.

Fricker HA, Hyland G, Coleman R *et al.* (2000b): Digital elevation models for the Lambert Glacier-Amery Ice Shelf system, East Antarctica, from ERS-1 satellite radar altimetry. Journal of Glaciology, 46(155): 553–560.

Fricker HA, Popov S, Allison I *et al.* (2001): Distribution of marine ice beneath the Amery Ice Shelf. Geophysical Research Letters, 28(11): 2241–2244.

Grosfeld K, Allison I, Craven M *et al.* (1998): Marine ice beneath Filchner Ice Shelf from a muti-disciplinary approach. in Ocean, Ice, and Atmosphere: Interactions at the Antarctic Continental Margin, Antarctic Research Series, 75: 319–339.

Jezek KC (1999): Glaciological properties of the Antarctic ice sheet from RADARSAT-1 synthetic aperture radar imagery. Annals of Glaciology, 29: 286–290.

Jezek KC (2003): Observing the Antarctic Ice Sheet using the RADARSAT-1 synthetic aperture radar, Polar Geography, 27(3): 197–209.

Liu H, Jezek KC, Li B (1999): Development of an Antarctic digital elevation model by integrating cartographic and remotely sensed data: A geographic information system based approach. Journal of Geophysical Research, 104(B10): 23199–23214.

Lythe MB, Vaughan DG (2001): the BEDMAP Consortium. BEDMAP: A new ice thickness and subglacial topographic model of Antarctica. Journal of Geophysical Research, 106(B6): 11335–11351.

Neal CS (1986): The dynamic of the Ross Ice Shelf revealed by radio echo-sounding. Geophysical Research Letters, 91: 756–762.

Rignot E (2002): East Antarctic glaciers and ice shelves mass balance from satellite data. Annals of Glaciology, 34: 228–234.

Rignot, E, Jacobs SS (2002): Rapid bottom melting widespread near Antarctic Ice Sheet grounding lines. Science, 296: 2020–2023.

Thyssen F, Bombosch A, Sandhager H (1993): Elevation, ice thickness and structure mark maps of the central part of the Filchner-Ronne Ice Shelf. Polarforschung, 62(1): 17–26.

Vaughan DG, Sievers J, Doake CSM *et al.* (1993): Subglacial and seabed topography, ice thickness and water column thickness in the vicinity of Filchner-Ronne-Schelfeis, Antarctica. Polarforschung, 64(2): 75–88.

Wang YF, Wen JH, Liu JY *et al.* (2006): Rapid change of the Antarctic Ice Sheet and glaciers. Chinese Journal of Polar Research, 18(1): 63–74.

Warren SG, Roesler CS, Morgan VI *et al.* (1993): Green icebergs formed by freezing of organic-rich seawater to the base of Antarctic ice shelves. Journal of Geophysical Research, 98(C4): 6921–6928.

Wen JH, Jezek KC, Csatho BM *et al.* (2006): Mass budgets of the Lambert, Mellor and Fisher glaciers and basal fluxes beneath their flowbands on Amery Ice Shelf. Science in China (Series D), submitted.

Williams MJM, Warner RC, Budd WF (1998): The effects of ocean warming and ocean circulation under the Amery Ice Shelf, East Antarctica. Annals of Glaciology, 27: 75–80.

Wong APS, Bindoff NL, Forbes A (1998): Ocean-ice shelf interaction and possible bottom water formation in Prydz Bay, Antarctica. in Ocean, Ice, and Atmosphere: Interactions at the Antarctic Continental Margin, Antarctic Research Series, 75: 173–187.

Zwally HJ, Schutz R, Bentley C *et al.* (2003): updated current year. GLAS/ICESat L2 Antarctic and Greenland Ice Sheet Altimetry Data V018, 15 October to 18 November 2003. Boulder, CO: National Snow and Ice Data Center. Digital media.